PROCEEDINGS REPRINT

SPIE—The International Society for Optical Engineering

Reprinted from

Application of Lidar to Current Atmospheric Topics

8–9 August 1996
Denver, Colorado

Volume 2833

Comparison of lidar water vapor measurements using Raman scatter at 266 nm and 532 nm

Franz Balsiger, C. Russell Philbrick

The Pennsylvania State University
Applied Research Laboratory
P.O. Box 30, State College, PA 16804
fxb9@psu.edu crp3@psu.edu

ABSTRACT

The performance of the **L**idar **A**tmospheric **P**rofile **S**ensor (LAPS) instrument for measurements of water vapor in the lower troposphere has been investigated. LAPS is an automated lidar system that measures water vapor from the vibrational Raman backscatter in the visible and in the ultraviolet wavelength range. We present a comparison of water vapor profiles measured with the lidar and balloon sondes as well as measured with the two lidar channels. With the UV channels it is possible to infer ozone profiles in the boundary layer. Data are presented that reveal the high variability of the water vapor in the boundary layer.

Keywords: Automated operational lidar, Raman scatter, water vapor, daytime measurements, ozone, troposphere.

1 INTRODUCTION

During the past twenty years, researchers at several laboratories have demonstrated that lidar has special capabilities for remote sensing of many different properties of the atmosphere. One of the techniques which shows a great deal of promise for several applications is Raman scattering. In this presentation, our application of the Raman scattering techniques to obtain profiles of water vapor and temperature in the lower atmosphere is described. The first Raman measurements of atmospheric properties with lidar were carried out in the late 1960's by Leonard and Cooney.[1,2] Two years later, Melfi, et al. and Cooney showed that it was possible to measure water vapor using the Raman lidar technique.[3,4,5] In 1972, a significant contribution was made by Inaba and Kobayasi in suggesting several species that could potentially be measured using vibrational Raman techniques.[6,7] While the early tests showed that it was possible to measure the water vapor with limited range and accuracy, recent investigations have shown significant improvements. Particularly, the investigations of Vaughan, et al., Melfi, et al., and Whiteman, et al. have demonstrated

0-8194-2221-5/96/$6.00

rather convincingly that the Raman technique has a high potential for making accurate water vapor measurements.[8,9,10] A most useful review of the Raman and DIAL lidar techniques applied to the water vapor measurement has been given by Grant.[11] The measurements of water vapor during the daytime have been demonstrated by Renaut and Capitini using the solar blind region of the ultraviolet spectrum.[12] Their work showed that the optimum wavelength for the measurement was near the fourth harmonic for the Nd:YAG laser. At this wavelength, the measurements of N_2 and H_2O are contaminated, at least to a small degree, by the absorption of ozone and SO_2 in the lower troposphere, however it appears that an adequate correction can be obtained from the use of the measured Raman signals of the N_2 and O_2 compared to their known mixing ratio.

2 INSTRUMENT

The **L**idar **A**tmospheric **P**rofile **S**ensor (LAPS) was designed to be an automated system to measure water vapor and temperature in the lower troposphere in order to determine refractivity profiles.[13] The water vapor measurement is based on vibrational Raman scatter, the temperature measurement is based on rotational Raman scatter. LAPS consist of a console and a deck unit which are connected over a 23 m fiber optic cable. The laser beam diameter is expanded by a factor of five and sent into the sky coaxial to the telescope. The prime focus parabolic telescope has a 61 cm diameter. The back scattered return is focused on a 1 mm fiber optic cable and guided to the detector box on the back of the control unit. We measure the return of the atmospheric rotational Raman scatter at 530 nm and 528 nm and the vibrational Raman scatter from water vapor at 660 nm and 295 nm, from nitrogen at 607 nm and 284 nm, and from oxygen at 277 nm. All seven wavelengths are detected by photon counting photo multiplier tubes (PMT) and sampled with a 100 MHZ counting device, minute by minute. The data are collected with 75 m height resolution up to 12 km. An X–band radar with a 6° cone angle prevents any possible illumination of an air plane with the beam.

3 DATA ANALYSIS

Raman lidar compares the return signals of the trace gas of interest, i.e. water vapor, with the Raman return of N_2. This ratio is proportional to the mixing ratio of the trace gas. The lidar equation describes the different factors that have an influence on the intensity of the return of a laser beam as a function of the range and the wavelength.[14] It is evident that taking the ratio of two wavelength eliminates all range dependent factors. Wavelength dependent factors, such as detector sensitivity, can be expressed as a calibration factor, however, wavelength and range dependent factors, such as transmission, must be corrected. First, the count rates of the different wavelengths are calculated by subtracting the measured background from the signal. Then, the count rates are corrected for saturation of the PMT's due to single overlap of consecutive pulses.[15] The count rates need to be corrected for the Rayleigh scattering of the atmosphere's molecules. In the lowest part of the atmosphere (< 5 km) a linear decreasing temperature can be assumed for the correction. The

Rayleigh correction is then given in an analytical way as a function of temperature and pressure at the ground and the temperature lapse rate.[16] The magnitude of the correction in the first 5 km is less than 1 % for the visible ratio and less than 10 % for the UV water vapor/nitrogen ratio. Since the UV ratio has to be corrected for tropospheric ozone (see the next section) with the oxygen/nitrogen ratio, the magnitude of the Rayleigh correction for the UV is reduced to the order of one percent.

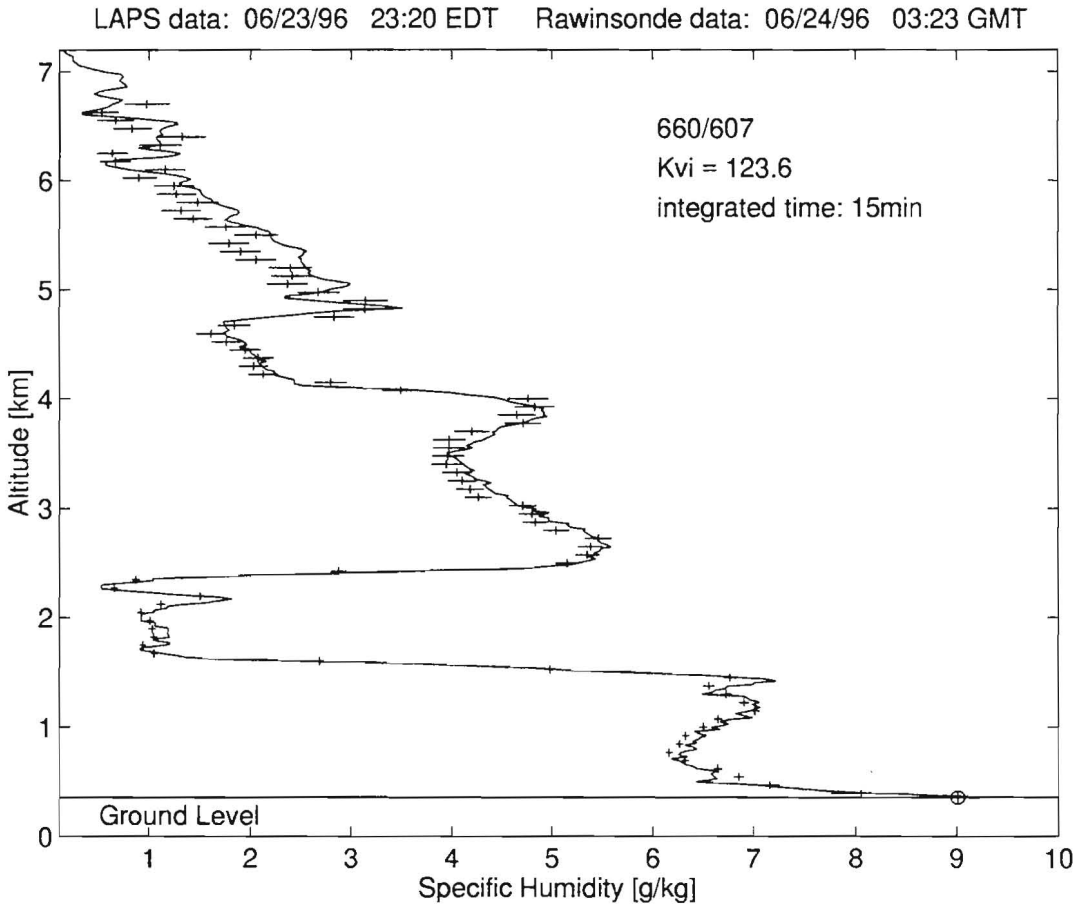

Figure 1: Comparison of a lidar water vapor profile (crosses with horizontal 1σ error bar, 15 min integration time) from the visible channel with a radiosonde profile (Vaisala RS 80–15). The data were taken on 23 June 1996 at 23:20 EDT in State College, PA. The circle at the ground is the humidity value measured by point sensors on the deck unit.

The specific humidity W_{vi} of the atmosphere derived from the visible channels is then given by the equation,

$$W_{vi}(z) = K_{vi} \times \frac{C_{H_2O}(z)}{C_{N_2}(z)}, \tag{1}$$

where K_{vi} is a calibration constant, $C_{H_2O}(z)$ and $C_{N_2}(z)$ are the count rates from the water vapor and nitrogen return as a function of the altitude. The calibration constant is determined by comparing the lidar ratio profile with a balloon profile as shown in Figure 1. We make a least square fit of Equation 1, taking in to account the statistical error of the lidar ratio and variance of

the balloon values over a lidar range bin (See section 5). The points corresponding to low water vapor (< 1 g/kg) and steep gradients are excluded from the determination of the calibration constant.

The count rates for the different channels are given as the difference between the measured signals and background counts for each of the channels. These quantities follow a Poisson distribution. For the calculation of measurement error we treat them as Gaussian distributed variables. This simplification leads to reasonable estimates of the measurement error. In Equation 1 (and later in Equation 3) the only critical term in the error propagation is the division by C_{N_2}. For $C_{N_2} < 5$ counts larger differences between the exact and the simplified technique would occur in the error estimation. Since we only look at data were C_{H_2O} is larger than 1 count and C_{N_2} is more than one order of magnitude larger than C_{H_2O} the critical condition never occurs.

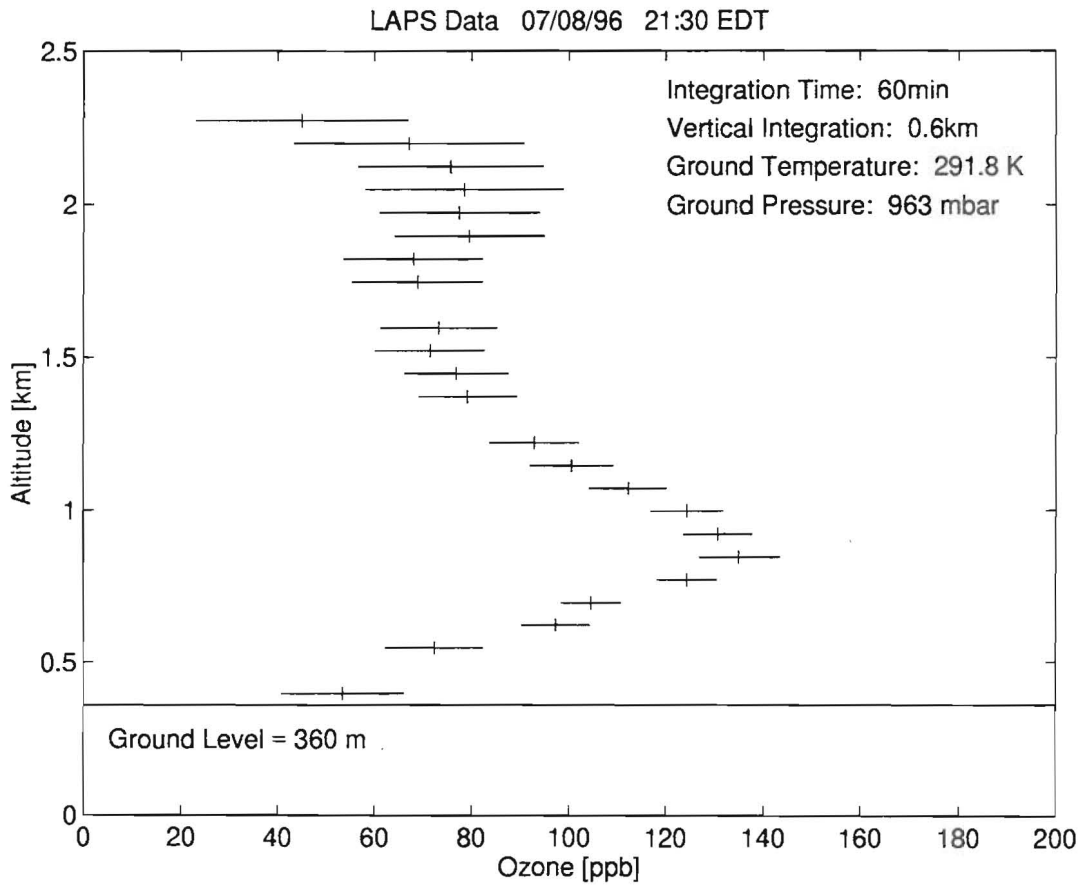

Figure 2: Ozone density measured on 8 July 1996 in State College, PA, where we have integrated data for one hour and the numerical derivative for each point is calculated over a height interval of 600 m. The measurement was made near the end of an ozone enhanced period.

4 OZONE CORRECTION

The derivation of the water vapor from the ultraviolet channels (UV) follows the same lines as shown in the previous section. Since the lines of the H_2O and N_2 Raman return are on the slope side of the Hartley band of ozone, the tropospheric ozone causes a differential absorption.[17] Therefore it is necessary to determine the ozone density O_3 in the measurement range. Applying the Beer–Lambert law for the oxygen and nitrogen returns leads to the following expression for the integrated ozone column density,

$$\frac{C_{O_2}(z)}{C_{N_2}(z)} = k \times \frac{O_2(z)}{N_2(z)} e^{-(\sigma_{O_2}-\sigma_{N_2})\int_0^z O_3(r)\,dr}, \tag{2}$$

where k is an instrumental constant and σ_{O_2} and σ_{N_2} are the absorption cross sections for ozone.[18] Since the ratio of O_2 and N_2 is constant in the homosphere, Equation 2 can be solved for the column density plus a height independent constant unknown offset. The derivative yields the ozone density, as shown in Figure 2. This ozone correction applied to the UV water vapor concentration is given by

$$W_{uv}(z) = K_{uv} \times \frac{C_{H_2O}(z)}{C_{N_2}(z)} \times \left[\frac{C_{O_2}(z)}{C_{N_2}(z)}\right]^{-\frac{\sigma_{H_2O}-\sigma_{N_2}}{\sigma_{N_2}-\sigma_{O_2}}}, \tag{3}$$

where C_x are the corresponding count rates and K_{uv} is the calibration constant for the UV channel. The influence of the ozone correction is shown in Figure 3. Since the nitrogen return is more strongly absorbed than the water return the ratio is overestimated with increasing altitude.

5 CALIBRATION CONSTANTS

In order to have an automated system it is important to know the calibration constant accurately and to maintain it as a stable value over a long period of time. An error of the calibration constant propagates linearly in the water vapor measurement. To obtain the calibration constant as mentioned in section 3, we compare the balloon data with the lidar profile by means of a least square fit. Since it takes about 30 min for the balloon to cross the altitude range of the lidar, it is difficult to decide what data of the balloon profile corresponds to which part of the lidar data. Not only the path of the balloon is different from the laser beam's vertical path, but also the atmosphere itself can change considerably over a short period of time as is shown in Figure 4. Although, such dramatic changes do not occur most of the time, in order to obtain the calibration constant we compare the balloon profile with six consecutive 10 min lidar profiles that are each five minutes apart and taken during the balloon's ascent. We then take the average of these six values as the calibration constant. In Table 1 we present the calibration constants for the visible and for the UV channel measured between 30 May and 8 July 1996. Over this period we achieve a stability of 7.5 % for the visible channel and 3.8 % for the UV channel.

6 COMPARISON

With its UV channels, which are in the solar blind spectral region, LAPS is designed to make daytime measurements. The question of weather the correction for tropospheric ozone is valid and

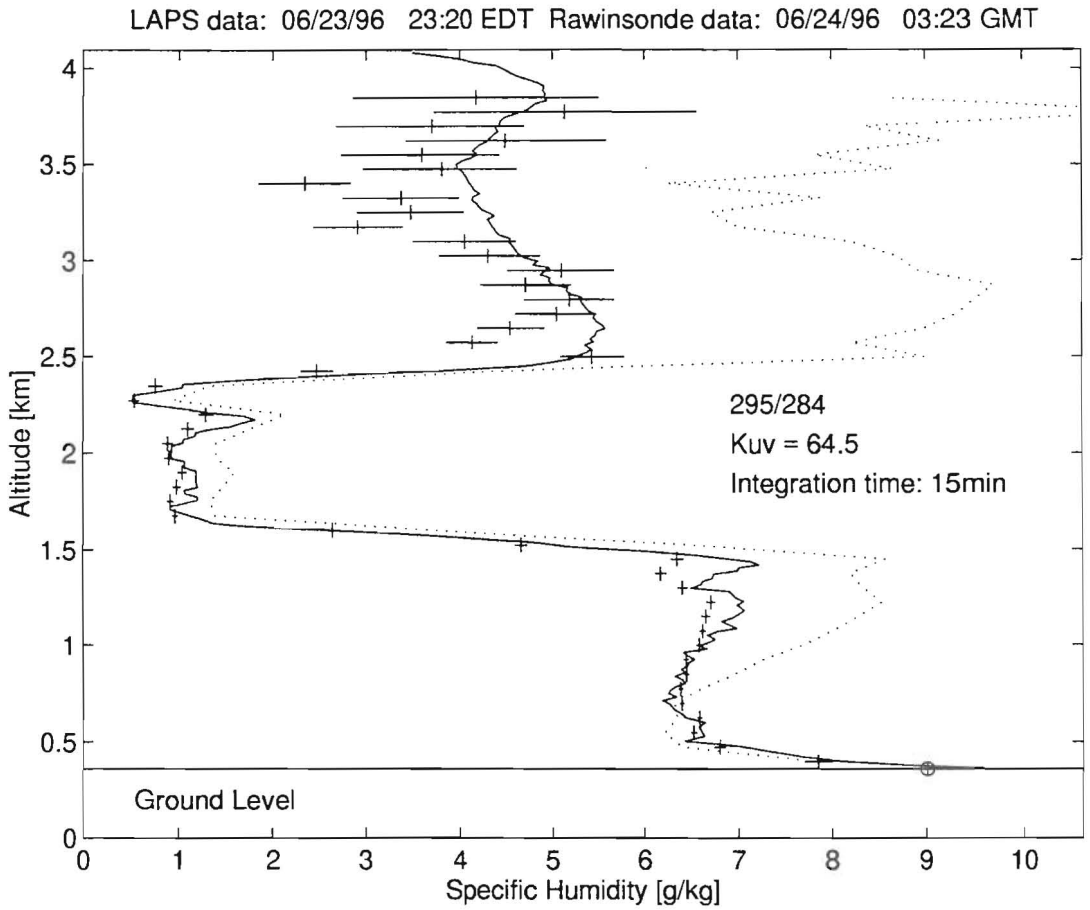

Figure 3: Comparison of a UV lidar water vapor profile (crosses with horizontal 1σ error bar, 15 min integration time) with a radiosonde profile (continuous line, Vaisala RS 80–15). The dotted line shows the UV profile without ozone correction. The data were taken on 23 June 1996 at 23:20 EDT in State College, PA. The circle at the ground is the humidity value measured on the deck unit. This UV data corresponds to the visible data profile shown in Figure 1.

sufficient has been investigated. As recognized by Renault et al., SO_2 will not contribute much to the differential absorption of these lines in the UV.[12] We have found that the water vapor derived from the visible and the UV channel are in good agreement. For the data presented earlier in Figure 4, a correlation analysis for the two channels has been made. Starting at 21:20 we have calculated seven consecutive pairs of 10 min profiles. These profiles are composed of data points with a relative error smaller than 30 %. The results from the correlation analysis are presented in Figure 5. Values from both wavelength regions are plotted against each other with their 1σ error bar. Generally the error bars are bigger for the UV because of the lower count rates. Although the water vapor mixing ratio can at times be highly variable, as shown in Figure 4, the correlation coefficient is as high as 0.989. The high correlation coefficient shows that the corrections applied to the UV data are valid and yield good results. This technique is therefore a valid approach to obtain daytime water vapor profiles in the boundary layer. In Figure 6 two daytime water vapor profiles measured on 13 March 1996 in State College, PA, are shown. Since it was a very dry winter day we have useful data only

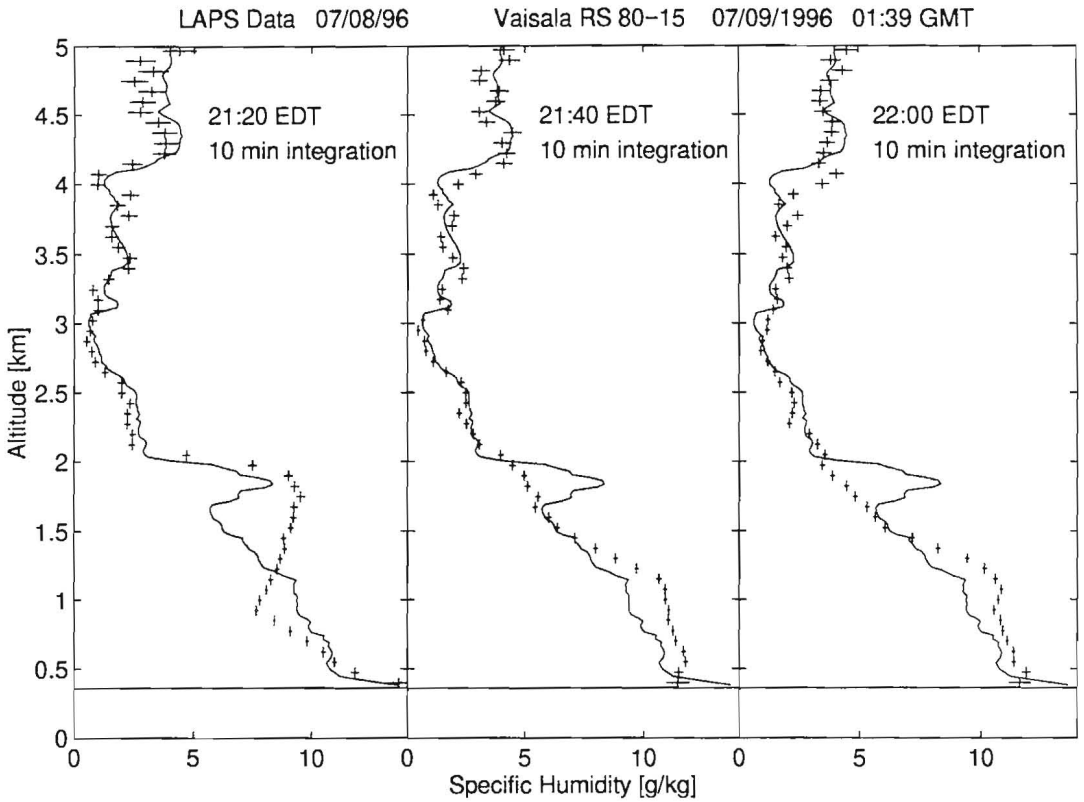

Figure 4: Atmospheric change of water vapor measured with the visible channel of LAPS . The profiles were taken on the evening of 8 July 1996 in State College, PA, each 20 min apart. For comparison a balloon profile measured at the same time is given in each of the panels.

up to 2 km. Under more humid conditions, as shown in Figure 3, we obtain profiles well above 3 km with a 15 min integration time. These two profiles are again an example for the high water vapor variability in the boundary layer.

7 SUMMARY

We have demonstrated the capability of LAPS to measure water vapor in the lower troposphere and in the boundary layer. LAPS measures water vapor with the Raman back scatter in the visible range and in the solar blind UV spectral region. A necessary correction for tropospheric ozone has been shown, which also gives the possibility to obtain ozone profiles in the first 2 km. A correlation analysis between the visible and the UV channels yield a high correlation coefficient of 0.989. We have shown two examples the high variability of the water vapor in the lower troposphere. Within less than 30 minutes large changes can occur which are described in high temporal (1 min) and vertical (75 m) resolution of LAPS . We have shown that we can maintain stable calibration constants within a few percent.

Date	Time	$K_{vi}[\frac{g}{kg}]\pm\sigma_{K_{vi}}$	$K_{uv}[\frac{g}{kg}]\pm\sigma_{K_{uv}}$
05/30/96	21:35	122.3±0.5	65.7±0.2
06/06/96	21:55	138.3±0.5	67.7±0.2
06/10/96	22:05	148.5±1.8	65.4±0.3
06/23/96	23:20	123.6±2.5	64.5±1.5
06/25/96	22:15	123.4±1.3	64.0±0.5
06/26/96	22:57	122.1±0.6	61.3±0.2
06/27/96	21:40	121.2±0.1	65.8±0.2
07/07/96	23:03	124.6±0.6	67.7±0.5
07/08/96	21:39	121.2±3.3	70.0±1.4
Average		127.2±9.6	65.8±2.5

Table 1: Calibration constants for LAPS for the visible and UV water vapor channel measured between 30 May and 8 July 1996. The statistical variation of the average constant is 7.5 % for the visible and 3.8 % for the UV channel.

8 ACKNWLEDGEMENTS

Special appreciation for the support of this work goes to NCCOSC NRaD and SPAWAR PMW–185. The work of F. Balsiger was partly sponsored by the Swiss National Science Foundation. We thank E. F. Boone, M. J. Bregar, D. L. McDowell, G. Pancoast, T. M. Petach, D. B. Lysak and R. W. Smith for their efforts in building the system and their support in obtaining the data.

9 REFERENCES

1. D. A. Leonard, "Observation of Raman scattering from the atmosphere using a pulsed nitrogen ultraviolet laser," *Nature* 216, 142-143, 1967.

2. J. A. Cooney, "Measurements on the Raman component of laser atmospheric backscatter," *Appl. Phys. Lett.*, 12, 40-42, 1968.

3. S. H. Melfi., J. D. Lawrence Jr. and M. P. McCormick, "Observation of Raman scattering by water vapor in the atmosphere," *Appl. Phys. Lett.*, 15, 295-297, 1969.

4. J. A. Cooney, "Remote measurement of atmospheric water vapor profiles using the Raman component of laser backscatter," *J. Appl. Meteor.*, 9, 182-184, 1970.

5. J. A. Cooney, "Comparisons of water vapor profiles obtained by rawinsonde and laser backscatter," *J. Appl. Meteor.*, 10, 301-308, 1971.

6. H. Inaba and T. Kobayasi, "Laser-Raman Radar," Opto-electronics, 4, 101-123, 1972.

7. R. G. Strauch, V. E. Derr and R. E. Cupp, "Atmospheric water vapor measurement by Raman lidar," *Remote Sens. Envir.* 2, 101-108, 1972.

8. G. Vaughan, D. P. Wareing, L. Thomas and V. Mitev, "Humidity measurements in the free troposphere using Raman backscatter," *Q. J. R. Meteorol. Soc.*, 114, 1471-1484, 1988.

9. S. H. Melfi, D. Whiteman and R. Ferrare, "Observations of atmospheric fronts using Raman lidar moisture measurements," *J. Appl. Meteo.*, 28, 789-806, 1989.

10. D. N. Whiteman, S. H. Melfi and R. A. Ferrare, "Raman lidar system for the measurement of

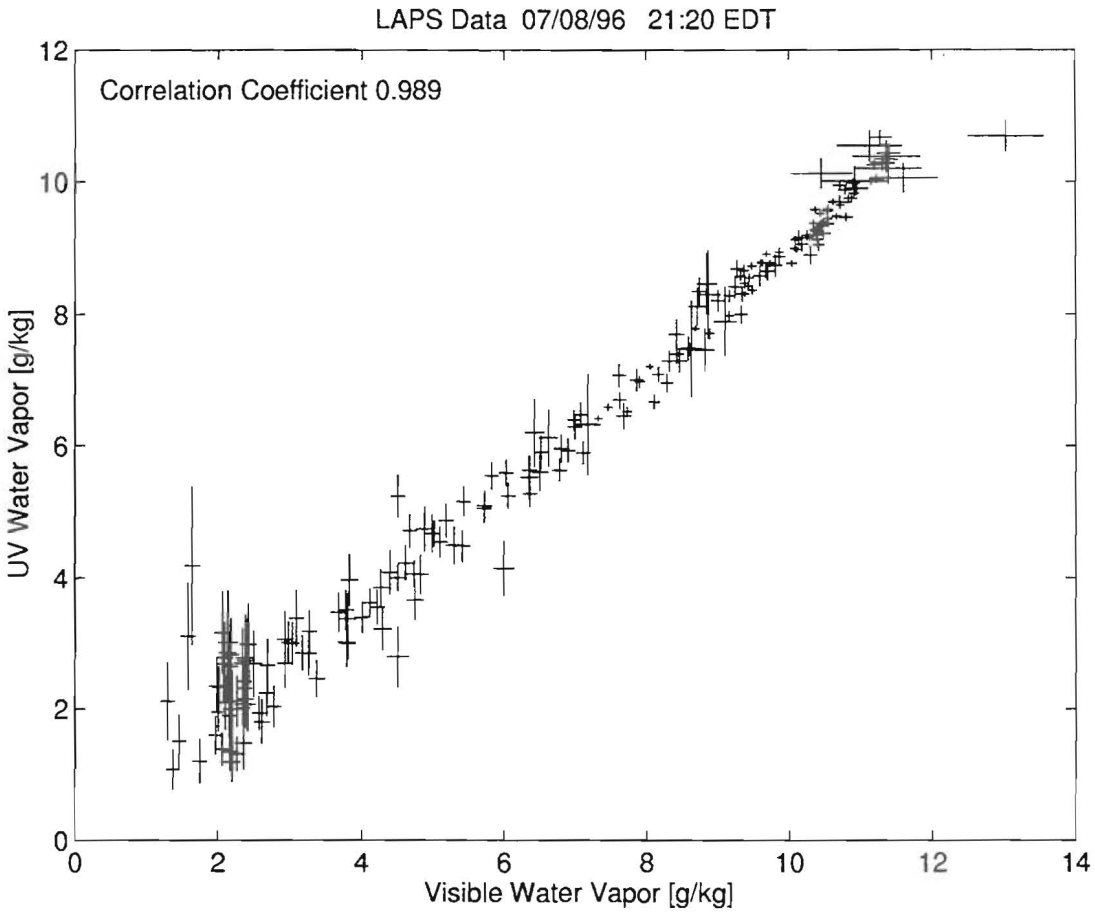

Figure 5: Correlation between the visible and the UV water vapor measured by LAPS. Starting at 21:20 EDT seven consecutive pairs of profiles are compared, each integrated over 10 min. During this period, strong variations in the water vapor profiles were observed (see Figure 4), nevertheless, the correlation coefficient is as high as 0.989.

water vapor and aerosols in the Earth's atmosphere," *Appl. Optics* 31, 3068-3082, 1992.

11. W. B. Grant, "Differential absorption and Raman lidar for water vapor profile measurements: a review," *Optical Engineering*, 30, 40-48, 1991.

12. D. Renaut and R. Capitini, "Boundary-layer water vapor probing with a solar-blind Raman lidar: validations, meteorological observations and prospects," *J. Atmos. Oceanic Tech.*, 5, 585-601, 1988.

13. C. R. Philbrick, "Raman lidar measurements of atmospheric properties," Atmospheric propagation and remote sensing III, SPIE Vol **2222**, 922–931, 1994.

14. R. M. Measures, *Laser Remote Sensing,* Chapter 7, Krieger Publishing Company, Malabar FL, 1992.

15. D. P. Donovan, J. A. Whiteway, and A. I. Carswell, "Correction for nonlinear photon–counting effects in lidar systems," *Applied Optics*, Vol. 32, No 33, 6742–6753, 1993.

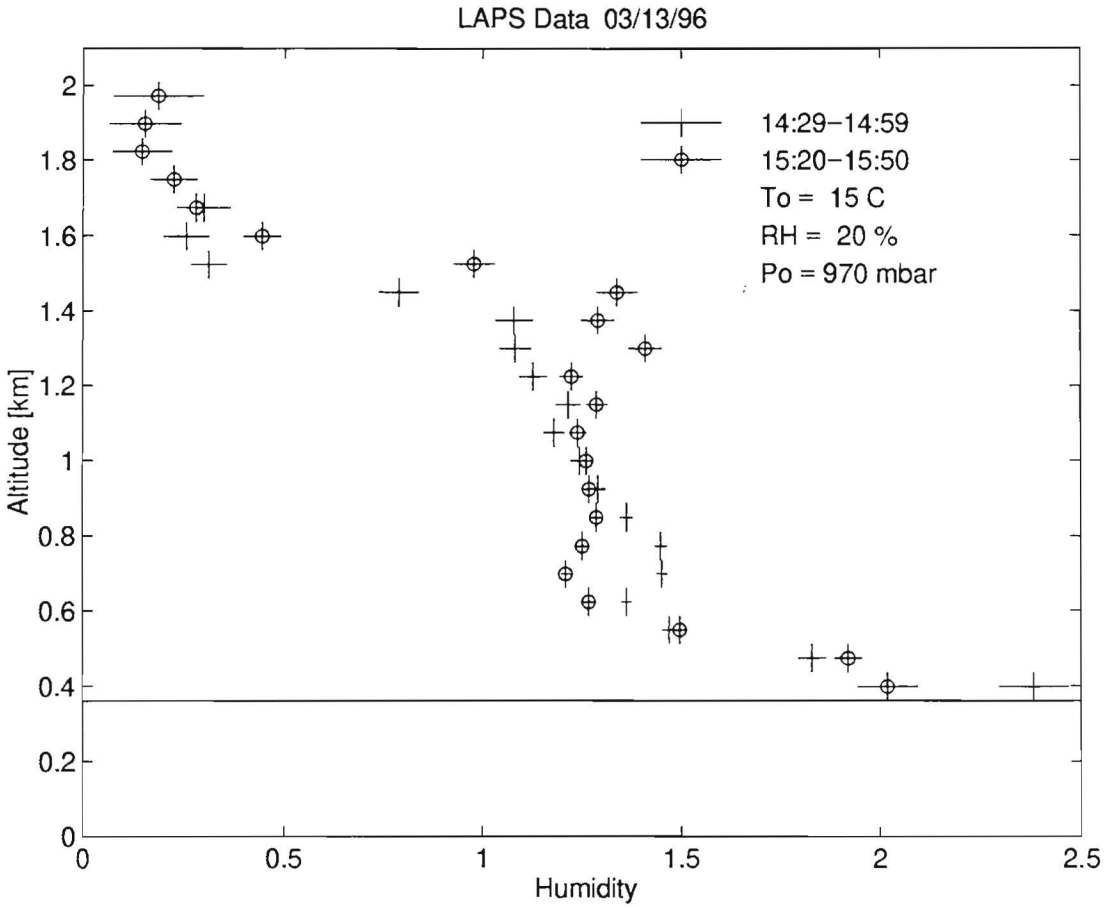

Figure 6: Two daytime water vapor profiles measured in State College, PA, on 13 March 1996, which show a considerable variation in the boundary layer profile.

16. R. Harris, F. Balsiger, C. R. Philbrick, "Comparison of lidar water vapor measurements using Raman scatter at 266 nm and 532 nm," *International Geoscience and Remote Sensing Symposium*, Vol. 3, 1826–1829, 1996.

17. D. Renault, J. C. Pourney, R. Capitini, "Daytime Raman–lidar measurements of water vapor," *Optics Letters*, Vol. 5, No. 6, 233–235, 1980.

18. L. T. Molina and M. J. Molina, "Absolute ozone cross sections of ozone in the 185– to 350 nm wavelength range," *J. Geophys. Res.*, Vol. 91, No D13, 14501–14508, 1986.